Comparison and Integration of GPS and SAR Data

M. Calamia[1], G. Franceschetti[2,3], R. Lanari[4], F. Casu[4,5], M. Manzo[4,6]

[1] Dipartimento Elettronica e Telecomunicazioni, Università di Firenze,
Via di Santa Marta 3, 50139 Firenze, Italy
[2] Dipartimento di Ingegneria Elettronica e delle Telecomunicazioni,
Università degli studi di Napoli Federico II, Via Claudio 21, 80125 Napoli, Italy
[3] University of California at Los Angeles (UCLA), USA
[4] Istituto per il Rilevamento Elettromagnetico dell'Ambiente (IREA),
National Research Council of Italy (CNR), Via Diocleziano 328, 80124 Napoli, Italy
[5] Dipartimento di Ingegneria Elettrica ed Elettronica,
Università degli studi di Cagliari, Piazza d'Armi, 09123 Cagliari, Italy
[6] Dipartimento di Ingegneria e Fisica dell'Ambiente, Università degli Studi della
Basilicata, Viale dell'Ateneo Lucano 10, 85100 Potenza, Italy

Abstract. We compare the surface deformation measurement capability of the Differential Synthetic Aperture Radar Interferometry (DIFSAR) technique, referred to as the Small BAseline Subset (SBAS) approach, and of the continuous Global Positioning System (GPS). The analysis is focused on the Los Angeles (California) test area where different deformation phenomena are present and a large amount of SAR data, acquired by the European Remote Sensing Satellite (ERS) sensors, and of continuous GPS measurements is available. The carried out analysis shows that the SBAS technique allows to achieve an estimate of the single displacement measurements, in the radar line of sight (LOS), with a standard deviation of about 5mm, which is comparable with the LOS-projected GPS data accuracy. Final remarks on the complementariness and integration of the SAR and GPS measurements are also provided.

1 SAR and GPS Data Comparison in the Los Angeles (California) Area

The Global Positioning System, usually referred to with the acronym GPS [1], is a fully-operational satellite navigation system based on a constellation of more than 24 GPS satellites; they broadcast precise timing signals via radio to the GPS receivers, allowing them to accurately determine their location (longitude, latitude, and altitude) with any weather, during day or night and everywhere on the Earth. GPS has become a global utility, indispensable for modern navigation on land, sea, and air around the world, as well as an important tool for map-making and land surveying. GPS also provides an extremely precise time reference, required for telecommunications and some scientific research. Among all these possible uses, the GPS data are also widely employed in geophysical applications to detect and follow the deformations of the Earth surface on a millimeter/centimeter scale, via the differential operational mode [1]. In the near future, the advanced European GA LILEO Positioning System will be operational.

More recently, the remote sensing technique referred to as Differential Synthetic Aperture Radar Interferometry (DIFSAR) has been developed [2], that also allows to investigate surface deformation phenomena on a millimeter/centimeter scale. In this case, it is exploited the phase difference (usually referred to as the interferogram) of two SAR images relevant to temporally separated observations of an investigated area. An effective procedure to detect and follow the temporal evolution of deformations is via the generation of time series; to achieve this task the information available from each interferometric data pair must be properly related to those included in the other acquisitions by generating an appropriate sequence of DIFSAR interferograms.

Several approaches aimed at the DIFSAR time series generation have been proposed. In this work, we focus on the technique referred to as the Small BAseline Subset (SBAS) algorithm [3], that has been originally developed to investigate large spatial scale displacements with relatively low resolution (typically of the order of 100×100 m). The SBAS approach relies on an appropriate combination of differential SAR interferograms characterized by small spatial and temporal separations between the orbits (baseline). As a consequence, the SAR data involved in the interferograms generation are usually grouped in several independent small baseline subsets, separated by large baselines. A way to easily "link" such subsets is the application of the Singular Value Decomposition (SVD) method.

The capability of the SBAS approach to generate deformation maps and time series from data acquired by the European Remote Sensing Satellite (ERS) sensors have been already shown in different applications [4, 5, 6]: an analysis on the quality of the DIFSAR measurements and comparison with geometric leveling and GPS techniques has been provided [7]. Accordingly, we focus in this presentation to the comparison between the SBAS-DIFSAR results and the measurements available from continuous GPS data. In particular, the investigated test site is the Los Angeles metropolitan zone (Southern California, USA), a tectonically active region with surface deformations caused by a variety of natural and anthropogenic actions. We remark that a key element for the seismic surveillance on the whole area is represented by the Southern California Integrated GPS Network (SCIGN) [8], which is an array of 250 GPS stations spread out across Southern California and northern Baja California, Mexico.

For what concerns the presented DIFSAR analysis, the SBAS algorithm has been applied to a set of 42 SAR data (track: 170, frame: 2925), acquired by the ERS satellites during the 1995–2002 time interval and coupled to 102 interferograms. Each interferometric SAR image pair has been chosen with a perpendicular baseline value smaller than 300 m and with a maximum time interval of 4 years; precise satellite orbital information and a Shuttle Radar Topography Mission (SRTM) Digital Elevation Model (DEM) [9] of the area have also been used. All the DIFSAR products have been obtained following a complex multilook operation [10] with 20 looks in the azimuth direction and 4 looks in the range one, with a resulting pixel dimension of the order of 100×100 m.

As a first result of the SBAS algorithm analysis, we present in Fig. 1a the geocoded SAR amplitude image relevant to the investigated area, with superimposed the retrieved line of sight (LOS) mean displacement velocity map and the locations of the GPS SCIGN sites (black and white squares) within the region.

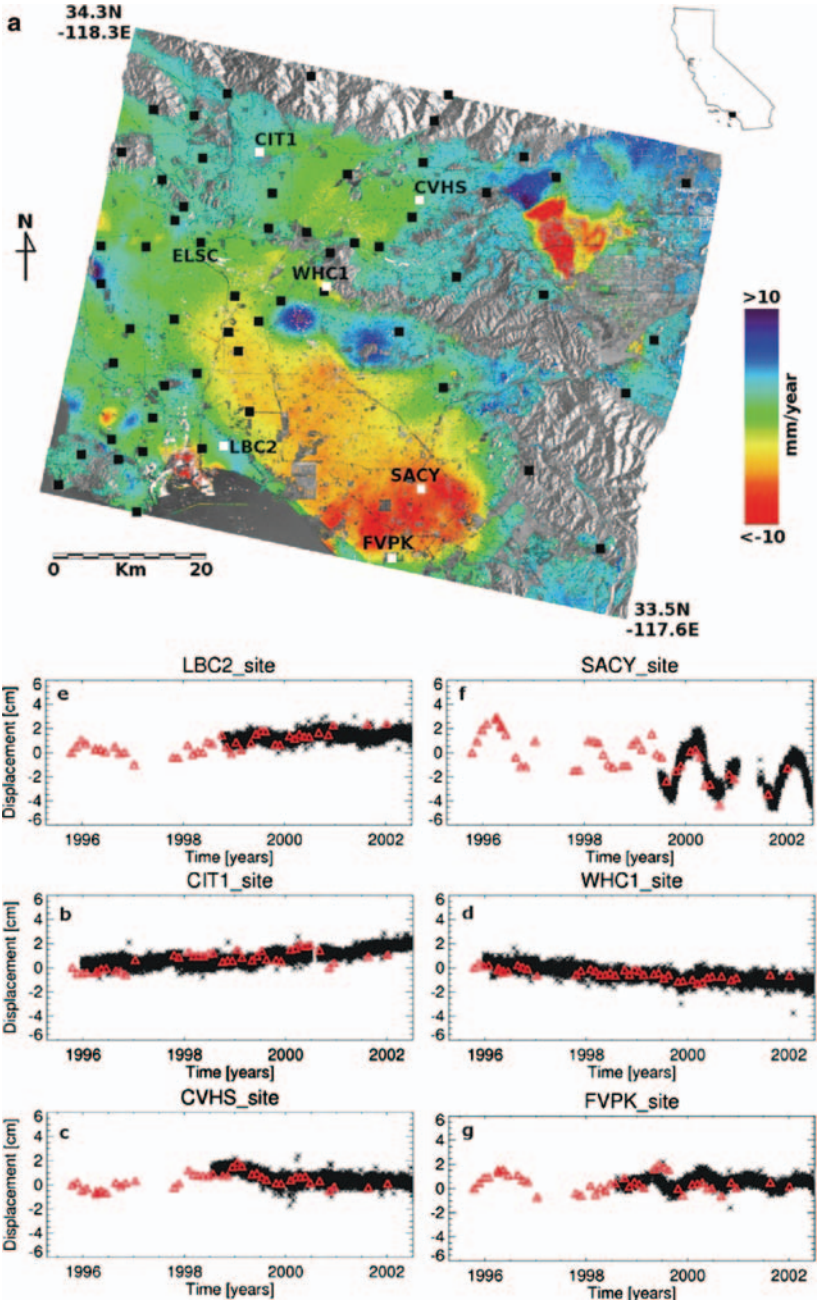

Fig. 1. DIFSAR results relevant to Los Angeles (California) metropolitan area. a) LOS mean deformation velocity map with superimposed the locations of the investigated GPS stations (black and white squares). White squares mark the selected stations relevant to the plots shown in Figs. 1b-g; the label ELSC identifies the reference point for both DIFSAR and geodetic measurements. b-g) Comparison between the DIFSAR LOS deformation time series (triangles) and the corresponding GPS measurements projected on the radar LOS (black stars), for the pixels labeled in Fig. 1a as CIT1, CVHS, WHC1, LBC2, SACY and FVPK, respectively.

Note that, we selected in our analysis the GPS stations located in coherent areas, and for which the measurements are relevant to a time interval starting before the year 2000 (in order to ensure at least two years of overlap with the available SAR data).

Following the mentioned GPS selection, we have compared the DIFSAR time series with the corresponding LOS-projected GPS measurements, the latter obtained through the SCIGN web site [11]. As first result of this comparison we show in Figs. 1b-g the plots relevant to the DIFSAR and GPS measurements for six sample GPS stations identified in Fig. 1a by the white squares and labeled as CIT1, CVHS, WHC1, LBC2, SACY and FVPK, respectively. Note that both DIFSAR and geodetic measurements have been referred to the same pixel located in correspondence of the ELSC station (see Fig. 1a). The presented results clearly show the good agreement between these two measurements.

Let us now move from a qualitative to a quantitative analysis. Accordingly, we have computed the standard devition values of the differences between the DIFSAR and the LOS-projected GPS time series for each GPS site identified by black and white squares in Fig. 1a (see Table 1) and the average of all these values; in this case, we obtained $\sigma_{d_{SAR}} = 6.9$ mm. Subsequently, we computed the LOS-projected GPS errors available from the SCIGN web site [10] and removed the bias due to the estimated errors relevant to the geodetic measurements. Following this bias removal, we finally achieved the mean value $\sigma_{d_{SAR}} = 5.6$ mm for the standard deviation of the difference between DIGSAR and GPS data. We remark that this value is rather close to the standard deviation of LOS-projected GPS errors whose mean value, computed from the measurements of the right column of Table 1, corresponds to $\sigma_{d_{GPS}} = 4$ mm.

2 Conclusions and Future Developments

We have compared the surface deformation measurement capability of the SBAS-DIFSAR technique and of continuous GPS. The analysis has been focused on the Los Angeles (California) test area and involved 42 SAR images, acquired by the ERS sensors in the 1995–2002 time interval, and continuous GPS measurements relevant to 38 sites. The carried out analysis has shown that the SBAS technique allows to achieve an estimate of the single displacement measurements with a standard deviation of about 5 mm. which is comparable with the LOS-projected GPS data accuracy.

As additional remark we underline that the integration of DIFSAR and GPS (and GALILEO soon) measurements is foreseen in future developments. Indeed, the former technique may provide spatially dense measurements but limited to a single component of the detected deformation phenomenon. On the contrary, the GPS (GALILEO) data are relevant to single points but allow to retrieve temporally dense time series with fully 3D information. The complementariness of the two techniques is evident.

A convenient possibility is the use of GPS (GALILEO) data as “tie points” at the DIFSAR phase-unwrapping stage. This renders the procedure overdetermined and appropriate processing techniques may be implemented to improve the accuracy of the solution. Forthcoming constellation SAR satellites will drastically reduce the

Table 1. Results of the compariosn between SAR and LOS-projected GPS deformation time series. The values shown in the third column have been obtained by projecting along the radar line of sight the information relevant to the errors available form the SCIGN web site (http://www.scign.org/).

GPS stations	Standard deviation of the difference between SAR and los-projected GPS measurements [cm]	Los-projected GPS errors [cm]
AZU1	0.71	0.43
BGIS	0.48	0.38
BRAN	0.85	0.42
CCCO	0.68	0.37
CCCS	0.73	0.37
CIT1	0.70	0.38
CLAR	1.09	0.37
CRHS	0.41	0.37
CSDH	0.58	0.36
CVHS	0.53	0.38
DSHS	0.54	0.43
DYHS	0.49	0.37
ECCO	0.48	0.38
EWPP	0.61	0.37
FVPK	0.82	0.37
JPLM	0.93	0.41
LASC	0.76	0.37
LBC1	0.79	0.42
LBC2	0.59	0.37
LONG	0.90	0.43
LORS	0.81	0.39
LPHS	0.47	0.40
MHMS	1.13	0.50
NOPK	0.47	0.44
PMHS	0.50	0.38
PVHS	0.77	0.44
PVRS	0.77	0.40
RHCL	0.49	0.39
SACY	0.85	0.43
SNHS	0.72	0.39
SPMS	0.65	0.37
TORP	0.69	0.38
USC1	0.73	0.42
VTIS	0.80	0.40
VYAS	0.48	0.39
WCHS	0.49	0.39
WHC1	0.38	0.39
WHI1	0.20	0.39

revisiting time, thus allowing statistical analysis to possibly detect systematic errors. In addition, knowledge of the full deformation map, as provided by DIFSAR, allows to optimize the GPS (GALILEO) sensors location providing also appropriate hints to the development of geological models.

Acknowledgments

This work has been partially sponsored by the CRdC-AMRA, ASI and the (Italian) GNV. We thank ESA which had provided the ERS data of the Los Angeles zone through the WInSAR data archive in collaboration with dr. P. Lundgren, JPL, Caltech. The GPS measurements relevant to the SCIGN network have been achieved through the SCIGN web site (http://www.scign.org/). Moreover, the DEM of the investigated zone has been achieved through the SRTM archive while precise ERS-1/2 satellite orbit state vectors are courtesy of the TU-Delft, The Netherlands.

References

[1] Kaplan, E., Hegarty, C., *Understanding GPS: Principles and Applications, 2nd Edition*, Artech House, Boston, MA, 644 pages, ISBN 1580538940, 2005.

[2] Gabriel, A. K., Goldstein, R. M., Zebker, H. A., Mapping small elevation changes over large areas: Differential interferometry, *J. Geophys. Res.*, 94, pp. 9183–9191, 1989.

[3] Berardino, P., Fornaro, G., Lanari, R., Sansosti, E., A new Algorithm for Surface Deformation Monitoring based on Samll Baseline Differential SAR Interferograms, *IEEE Trans. Geosci. Rem. Sens.*, 40, 11, pp. 2375–2383, 2002.

[4] Lundgren, P., Casu, F., Manzo, M., Pepe, A., Berardino, P., Sansosti, E., Lanari, R., Gravity and magma induced spreading of Mount Etna volcano revealed by satellite radar interferometry, *Geoph. Res. Lett.*, 31, L04602, doi: 10.1029/2003GL018736, 2004.

[5] Lanari, R., Lundgren, P., Manzo, M., Casu, F., Satellite radar interferometry time series analysis of surface deformation for Los Angeles, California, *Geoph. Res. Lett.*, 31, L23613, doi:10.1029/2004GL021294, 2004.

[6] Borgia, A., Tizzani, P., Solaro, G., Manzo, M., Casu F., Luongo, G., Pepe, A., Berardino, P., Fornaro, G., Sansosti, E., Ricciardi, G. P., Fusi, N., Di Donna, G., Lanari, R., Volcanic spreading of Vesuvius, a new paradigm for interpreting is volcanic activity, *Geoph. Res. Lett.*, 32, L03303, doi:10.1029/2004GL022155, 2005.

[7] Casu, F., Manzo, M., Lanari, R., A Quantitative Assessment of the SBAS Algorithm Performance for Surface Deformation Retrieval from DIFSAR Data, in press on *Remote Sensing of Environment*, doi: 10.1016/j.rse.2006.01.023, 2006.

[8] Hudnut, K. W., Bock, Y., Galetzka, J. E., Webb, F. H., Young W. H., The Southern California Integrated GPS Network (SCIGN). *Proc. Of the The 10th FIG International Symposium on Deformation Measurements*, 19–22 March 2001 Orange, California, USA, pp. 129–148, 2001.

[9] Rosen, P. A., Hensley, S., Gurrola, E., Rogez, F., Chan, S., Marthin, J., SRTM C-band topographic data quality assessment and calibration activities, *Proc, of IGARSS'01*, pp. 739–741, 2001.

[10] Rosen, P. A., Hensley, S., Joughin, I. R., Li, F. K., Madsen, S. N., Rodriguez, E., Goldstein, R., Synthetic Aperture Radar Interferometry, *IEEE Proc.*, 88, pp. 333–376, 2000.

[11] SCIGN web site: http://www.scign.org/.